

SENSOR LOCALIZATION USING RADIO AND ACOUSTIC TRANSMISSIONS FROM A MOBILE ACCESS POINT

Richard J. Kozick¹, Brian M. Sadler², Chin-Chen Lee³, Lang Tong³

¹Bucknell University, Lewisburg, PA

²Army Research Laboratory, Adelphi, MD

³Cornell University, Ithaca, NY

ABSTRACT

We consider the problem of sensor node localization in a randomly deployed sensor network, using a mobile access point (AP). The mobile AP can be used to localize many sensors simultaneously in a broadcast mode, without a pre-established sensor network. We consider a multi-modal approach, combining radio and acoustics. The radio broadcasts timing, location information, and acoustic signal parameters. The acoustic emission may be used at the sensor to measure Doppler stretch, time delay, received signal strength, or angle of arrival. We focus on the case of narrowband Doppler shift in this paper, and we present a maximum likelihood estimator for sensor localization and show that its performance achieves the Cramér-Rao bound.

1. INTRODUCTION

Wireless sensor networks composed of low-cost, expendable, multimode sensors are a key part of the Army Future Combat Systems program to perform target detection, location, classification, and imaging. An accurate estimate of the location of each node in the network is needed in order to make use of the measured sensor data. Manual placement of the nodes at specific locations is impractical because sensor networks often contain a large number of nodes and the territory may be hostile, and including a GPS unit in each node is undesirable due to cost and energy consumption considerations. An approach to sensor localization that has been studied by several researchers, e.g., [1, 2], involves passing messages between the nodes. This approach requires the deployment of beacon nodes and/or anchor nodes with known location within the network, and it requires the communication network to be established before the nodes are localized.

We consider using a cooperative mobile access point (AP) that is external to the network to perform the communication, beacon, and anchor functions. This approach allows each sensor node to determine its own location without requiring communication or clock synchronization between the nodes. Nodes can be localized at the time they are deployed (the mobile AP may deploy the nodes), when new nodes are added to an existing network, or when the nodes in a network are moved. Uplink communications

may be desirable to request more beaconing from the AP to reduce the localization error to a desired tolerance. Acoustic experiments with a helicopter as the mobile AP are reported in [3].

The sensor localization scheme works as follows. The AP is assumed to have an accurate estimate of its own location and motion (e.g., from GPS), and each sensor node is assumed to contain a microphone (among other sensors), a signal processor, and a low-bandwidth, low-power radio. The AP broadcasts simultaneous acoustic and radio signals from multiple beaconing positions. The radio signal carries information about the AP location and motion, timing, and parameters of the acoustic signal. The acoustic signal is designed so that it can be measured at the sensor node and processed to estimate a quantity such as Doppler shift, time delay (TD), received signal strength (RSS), or angle of arrival (AOA). The sensor node then estimates its location by combining the information from the radio and acoustic signals.

Node localization may be performed using a single transmission modality from the mobile AP, but combining radio and acoustics makes better use of the sensor node resources. Using radio alone to estimate Doppler, TD, or AOA requires a more sophisticated radio than is typically found in low-cost sensor nodes. Using acoustics alone to estimate Doppler, TD, or AOA requires the nodes to communicate with each other as in [1]. Combining radio and acoustics eliminates communication between the nodes and simplifies the signal processing for node localization since the AP locations and acoustic signal parameters are known.

In this paper, we consider self-localization of sensors based on measuring the acoustic Doppler shift in a tone that is emitted from a mobile AP at several locations. We assume that the AP location and heading as well as the frequency of the acoustic tone are known at the sensor node (via the radio signal). Sensor localization using Doppler shift is attractive because it requires only one microphone and the processing is very simple (spectral line estimation).

An outline of the paper is as follows. We begin with a model for the Doppler-shifted acoustic tone measured at the sensor node. The Cramér-Rao bound (CRB) on sensor localization accuracy and the maximum likelihood (ML) estimator of sensor location are then presented, followed

Report Documentation Page				Form Approved OMB No. 0704-0188	
Public reporting burden for the collection of information is estimated to average 1 hour per response, including the time for reviewing instructions, searching existing data sources, gathering and maintaining the data needed, and completing and reviewing the collection of information. Send comments regarding this burden estimate or any other aspect of this collection of information, including suggestions for reducing this burden, to Washington Headquarters Services, Directorate for Information Operations and Reports, 1215 Jefferson Davis Highway, Suite 1204, Arlington VA 22202-4302. Respondents should be aware that notwithstanding any other provision of law, no person shall be subject to a penalty for failing to comply with a collection of information if it does not display a currently valid OMB control number.					
1. REPORT DATE 01 NOV 2006		2. REPORT TYPE N/A		3. DATES COVERED -	
4. TITLE AND SUBTITLE Sensor Localization Using Radio & Acoustic Transmissions from a Mobile Access Point				5a. CONTRACT NUMBER	
				5b. GRANT NUMBER	
				5c. PROGRAM ELEMENT NUMBER	
6. AUTHOR(S)				5d. PROJECT NUMBER	
				5e. TASK NUMBER	
				5f. WORK UNIT NUMBER	
7. PERFORMING ORGANIZATION NAME(S) AND ADDRESS(ES) Bucknell University, Lewisburg, PA				8. PERFORMING ORGANIZATION REPORT NUMBER	
9. SPONSORING/MONITORING AGENCY NAME(S) AND ADDRESS(ES)				10. SPONSOR/MONITOR'S ACRONYM(S)	
				11. SPONSOR/MONITOR'S REPORT NUMBER(S)	
12. DISTRIBUTION/AVAILABILITY STATEMENT Approved for public release, distribution unlimited					
13. SUPPLEMENTARY NOTES See also ADM002075., The original document contains color images.					
14. ABSTRACT					
15. SUBJECT TERMS					
16. SECURITY CLASSIFICATION OF:			17. LIMITATION OF ABSTRACT UU	18. NUMBER OF PAGES 28	19a. NAME OF RESPONSIBLE PERSON
a. REPORT unclassified	b. ABSTRACT unclassified	c. THIS PAGE unclassified			

by results on sensor localization accuracy via analysis of the CRB for straight-line paths and Monte Carlo simulation of the ML estimator performance for more complex AP paths. Computer simulations indicate that the ML estimator achieves the performance of the CRB.

2. SYSTEM MODEL

The geometry of the mobile AP and sensor is illustrated in Figure 1. The unknown sensor location is denoted by $\tilde{\mathbf{x}}_0$, and the mobile AP locations and velocity vectors at N times are denoted by $\tilde{\mathbf{x}}_n$ and $\dot{\tilde{\mathbf{x}}}_n$, respectively, for $n = 1, \dots, N$. We assume that the sensor is in the $z = 0$ plane, i.e., its elevation is known, so the unknown part is \mathbf{x}_0 , defined as

$$\tilde{\mathbf{x}}_0 = \begin{bmatrix} x_0 \\ y_0 \\ 0 \end{bmatrix}, \quad \mathbf{x}_0 = \begin{bmatrix} x_0 \\ y_0 \end{bmatrix}. \quad (1)$$

We assume that the mobile AP elevation is constant at z , and define

$$\tilde{\mathbf{x}}_n = \begin{bmatrix} x_n \\ y_n \\ z \end{bmatrix}, \quad \mathbf{x}_n = \begin{bmatrix} x_n \\ y_n \end{bmatrix},$$

$$\dot{\tilde{\mathbf{x}}}_n = \begin{bmatrix} \dot{x}_n \\ \dot{y}_n \\ 0 \end{bmatrix}, \quad \dot{\mathbf{x}}_n = \begin{bmatrix} \dot{x}_n \\ \dot{y}_n \end{bmatrix}, \quad n = 1, \dots, N, \quad (2)$$

where vectors with \sim are in three dimensions. The mobile AP path is denoted by

$$\mathcal{P} = \{(\tilde{\mathbf{x}}_n, \dot{\tilde{\mathbf{x}}}_n), n = 1, \dots, N\}. \quad (3)$$

The radial vectors from AP to sensor are $\tilde{\mathbf{r}}_n = \tilde{\mathbf{x}}_0 - \tilde{\mathbf{x}}_n$, the range is $r_n = \|\tilde{\mathbf{r}}_n\|$, and the AP speed is $V_n = \|\dot{\tilde{\mathbf{x}}}_n\|$. The mobile AP emits an acoustic tone with frequency f_s Hz, so the Doppler-shifted frequency observed at the sensor is

$$f_n = f_s + \left(\frac{f_s}{c}\right) \frac{(\dot{\tilde{\mathbf{x}}}_n^T \tilde{\mathbf{r}}_n)}{r_n} \quad (4)$$

$$= f_s + \left(\frac{f_s}{c}\right) \frac{\dot{x}_n(x_0 - x_n) + \dot{y}_n(y_0 - y_n)}{[(x_0 - x_n)^2 + (y_0 - y_n)^2 + z^2]^{1/2}} \quad (5)$$

$$= f_s + \left(\frac{f_s}{c}\right) g(\mathbf{x}_0; \tilde{\mathbf{x}}_n, \dot{\tilde{\mathbf{x}}}_n), \quad n = 1, \dots, N, \quad (6)$$

where c is the speed of sound. In (4)-(6), the sensor location \mathbf{x}_0 is unknown and the quantities $f_s, c, x_n, y_n, z, \dot{x}_n, \dot{y}_n$ are known because they are transmitted via radio from the mobile AP. The speed of sound can be estimated from measurements of meteorological parameters such as temperature, humidity, and so on; e.g., see [9]. The function

$g(\mathbf{x}_0; \tilde{\mathbf{x}}_n, \dot{\tilde{\mathbf{x}}}_n)$ is defined in (6) to emphasize that the sensor location \mathbf{x}_0 is unknown while the AP parameters $\tilde{\mathbf{x}}_n, \dot{\tilde{\mathbf{x}}}_n$ are known.

The sensor node can estimate its location based on estimates of the Doppler shifts, $\Delta f_n \triangleq f_n - f_s$, by solving (5). The Doppler shift estimates at the sensor node will contain random errors caused by many factors, including sensor noise, atmospheric turbulence, and AP motion that produces time variations in the Doppler frequency. We have developed models and analyzed the effects of these errors, but the details are omitted in this paper. For example, we have shown that atmospheric turbulence has a significant impact on the accuracy of acoustic Doppler estimation [4, 5], and the effect of AP motion on Doppler frequency shift has been analyzed in [6]-[8]. For simplicity, we model the estimation errors with Gaussian random variables $\epsilon_1, \dots, \epsilon_N$ that are independent with zero-mean and known variance σ_n^2 , i.e., $\epsilon_n \sim \mathcal{N}(0, \sigma_n^2)$. The model for N measurements of the Doppler shift at the sensor node is then

$$\Delta f_n = \left(\frac{f_s}{c}\right) g(\mathbf{x}_0; \tilde{\mathbf{x}}_n, \dot{\tilde{\mathbf{x}}}_n) + \epsilon_n \quad (7)$$

$$\sim \mathcal{N}\left(\left(\frac{f_s}{c}\right) g(\mathbf{x}_0; \tilde{\mathbf{x}}_n, \dot{\tilde{\mathbf{x}}}_n), \sigma_n^2\right), \quad n = 1, \dots, N. \quad (8)$$

Figure 2 contains an illustration of the process of sensor localization via acoustic Doppler shift from a mobile AP.

The maximum likelihood (ML) estimate of sensor node location is given by weighted, nonlinear least-squares,

$$\hat{\mathbf{x}}_0 = \arg \min_{\mathbf{x}} \sum_{n=1}^N \frac{1}{\sigma_n^2} \left[\Delta f_n - \left(\frac{f_s}{c}\right) g(\mathbf{x}; \tilde{\mathbf{x}}_n, \dot{\tilde{\mathbf{x}}}_n) \right]^2. \quad (9)$$

The Fisher Information Matrix (FIM) for a given path \mathcal{P} as defined in (3) with respect to the sensor location \mathbf{x}_0 is [10]

$$\mathbf{J}(\mathbf{x}_0|\mathcal{P}) = \sum_{n=1}^N \frac{1}{\sigma_n^2} \left(\frac{\partial \Delta f_n}{\partial \mathbf{x}_0} \right) \left(\frac{\partial \Delta f_n}{\partial \mathbf{x}_0} \right)^T, \quad (10)$$

where the gradient vectors have the form

$$\frac{\partial \Delta f_n}{\partial \mathbf{x}_0} = \frac{f_s}{c} \frac{1}{r_n} \left(\dot{\tilde{\mathbf{x}}}_n - \frac{(\dot{\tilde{\mathbf{x}}}_n^T \tilde{\mathbf{r}}_n)}{r_n^2} (\mathbf{x}_0 - \mathbf{x}_n) \right). \quad (11)$$

The Cramér-Rao bound (CRB) on the variance of unbiased estimates of the sensor location are given by the diagonal elements of \mathbf{J}^{-1} , provided that \mathbf{J} is nonsingular. Singularity of the FIM is related to identifiability of \mathbf{x}_0 in the model (7), where if the model is not locally identifiable, then the FIM is singular and the CRB is not always defined [11]. Whether or not the FIM is singular depends on the mobile AP path \mathcal{P} in (3) and the sensor location \mathbf{x}_0 . We define

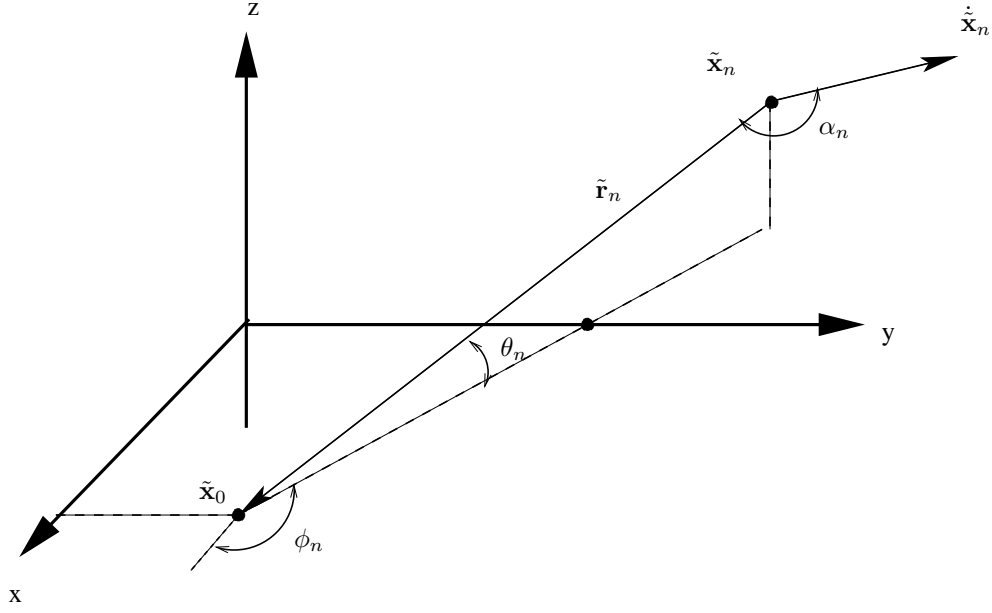


Fig. 1. Geometry of sensor at $\tilde{\mathbf{x}}_0$ and mobile AP at location $\tilde{\mathbf{x}}_n$ with velocity $\dot{\tilde{\mathbf{x}}}_n$.

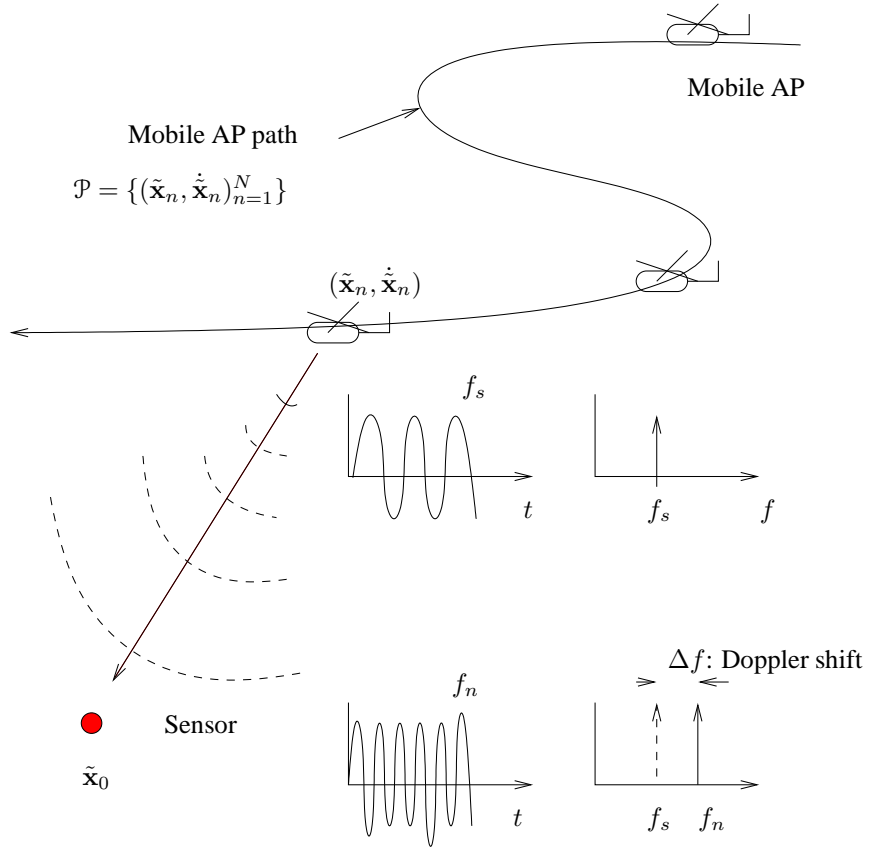


Fig. 2. Illustration of sensor localization using acoustic Doppler shift from a mobile AP.

the set of sensor positions that are *unlocalizable* for a given path \mathcal{P} as

$$\mathcal{X}(\mathcal{P}) = \{\mathbf{x} \mid \det(\mathbf{J}(\mathbf{x}|\mathcal{P})) = 0\}. \quad (12)$$

It is clear from (10) that all sensor positions are unlocalizable for $N = 1$ transmission from the mobile AP. Straight line AP paths will be analyzed with respect to (12) in the next section.

3. ANALYSIS OF SENSOR LOCALIZABILITY

We analyze Doppler-based localizability of a sensor position when the mobile AP travels at constant velocity in a straight line. We prove that the set of unlocalizable sensor positions is the line directly underneath the AP path as long as the mobile AP transmits from $N \geq 2$ distinct positions. The proof follows from a matrix factorization of the FIM for the sensor position parameters. The FIM of a given path \mathcal{P} with respect to sensor position \mathbf{x}_0 is given in (10), with the gradient vectors defined in (11). The set of unlocalizable sensor positions for a given path \mathcal{P} is defined as the set $\mathcal{X}(\mathcal{P})$ in (12).

Consider an AP path with *constant velocity* \mathbf{v} and *constant height* z , so the AP position and velocity vectors are defined as in (2), and we define the AP speed as $V = \|\mathbf{v}\|$. If we define \mathbf{b} as a unit-length vector that is orthogonal to the velocity vector \mathbf{v} , so $\mathbf{v}^T \mathbf{b} = 0$ and $\|\mathbf{b}\| = 1$, then the AP path is characterized by parameters $\alpha = [\alpha_1, \dots, \alpha_N]^T$ and β ,

$$\mathcal{P}(\mathbf{v}, \mathbf{b}, z, \alpha, \beta) = \left\{ \left(\tilde{\mathbf{x}}_n, \dot{\tilde{\mathbf{x}}}_n \right)_{n=1}^N \mid \dot{\tilde{\mathbf{x}}}_n = \begin{bmatrix} \mathbf{v} \\ 0 \end{bmatrix}, \right. \\ \left. \tilde{\mathbf{x}}_n = \begin{bmatrix} \alpha_n \mathbf{v} + \beta \mathbf{b} \\ z \end{bmatrix} \right\}. \quad (13)$$

The set of unlocalizable sensor positions for the constant velocity, constant height path in (13) is the line directly underneath the AP path,

$$\mathcal{X}(\mathcal{P}(\mathbf{v}, \mathbf{b}, z, \alpha, \beta)) = \{t\mathbf{v} + \beta\mathbf{b}, t \in \mathbb{R}\}. \quad (14)$$

An outline of the proof is given next.

We begin by representing a sensor position \mathbf{x}_0 by two parameters (t_0, s_0) that are its components along the AP velocity vector \mathbf{v} and orthogonal to \mathbf{v} ,

$$\mathbf{x}_0 = t_0 \mathbf{v} + s_0 \mathbf{b}. \quad (15)$$

Then it can be shown that the FIM in (10) has the following form for \mathbf{x}_0 in (15),

$$\mathbf{J}((t_0, s_0) | \mathcal{P}) = \left(\frac{f_s}{c} \right)^2 \begin{bmatrix} \mathbf{v} & -\mathbf{b} \end{bmatrix} \mathbf{A} \mathbf{W} \mathbf{A}^T \begin{bmatrix} \mathbf{v}^T \\ -\mathbf{b}^T \end{bmatrix}, \quad (16)$$

where the matrix $\mathbf{A} = [\mathbf{a}_1, \dots, \mathbf{a}_N]$ has columns

$$\mathbf{a}_n = \begin{bmatrix} (s_0 - \beta)^2 + z^2 \\ (t_0 - \alpha_n) V^2 (s_0 - \beta) \end{bmatrix}, \quad (17)$$

\mathbf{W} is the diagonal matrix

$$\mathbf{W} = \text{diag} \left\{ \frac{1}{\sigma_1^2 r_1^6}, \dots, \frac{1}{\sigma_N^2 r_N^6} \right\}, \quad (18)$$

and r_n is defined as

$$r_n^2 = (t_0 - \alpha_n)^2 V^2 + (s_0 - \beta)^2 + z^2. \quad (19)$$

We assume that $r_n > 0$, $n = 1, \dots, N$ (the AP is never in the same location as the sensor). The matrices $\begin{bmatrix} \mathbf{v} & -\mathbf{b} \end{bmatrix}$ and \mathbf{W} in (16) are full rank, so $\text{rank } \mathbf{J}((t_0, s_0) | \mathcal{P}) = \text{rank } \mathbf{A}$. We can examine the conditions for \mathbf{A} to have rank 2 by computing the determinant of two distinct columns m and n of \mathbf{A} ,

$$\det \begin{bmatrix} (s_0 - \beta)^2 + z^2 & (s_0 - \beta)^2 + z^2 \\ (t_0 - \alpha_m) V^2 (s_0 - \beta) & (t_0 - \alpha_n) V^2 (s_0 - \beta) \end{bmatrix} \\ = [(s_0 - \beta)^2 + z^2] (s_0 - \beta) V^2 (\alpha_m - \alpha_n). \quad (20)$$

We assume that the source is moving ($V > 0$), so $\alpha_m \neq \alpha_n$. Therefore the determinant in (20) equals 0 if and only if $s_0 = \beta$, which by (15) is equivalent to the sensor position $\mathbf{x}_0 \in \mathcal{X}(\mathcal{P}(\mathbf{v}, \mathbf{b}, z, \alpha, \beta))$ in (14).

4. SIMULATION EXAMPLES

We present two simulation examples of sensor localizability in which the performance of the ML estimator in (9) is compared to the CRB. In the first example, the AP flies in a circle at elevation $z_n = z = 100$ m (for all n) and various values for the radius of the circle, r_n . The AP transmits an acoustic tone from 40 equally-spaced locations along the circular path, where the tone has frequency $f_s = 100$ Hz and the AP speed is 33.5 m/s. The AP circle is centered at the origin, and the sensor location is moved along the x -axis, which is the abscissa in the plots of Figure 3. Note that in Figure 3, r_n is the radius of the circular AP path (and not range from the AP to the sensor as in (4) and (19)). Note that the ML estimator achieves the CRB, and localization accuracy on the order of meters (or less) is achieved as long as the sensor location is inside the circle of the AP path.

In the second example, the AP flies in a straight line at elevation $z_n = z = 100$ m (for all n). The AP path is along the y -axis at $x = 0$, with end-to-end distance of 1,000 m from $y = -500$ to 500 m. The AP transmits an acoustic tone from 40 equally-spaced locations along the path, where the tone has frequency $f_s = 100$ Hz and the AP speed is 33.5 m/s. The sensor location is moved along the x -axis at $y = 0$, which is the abscissa in the plots of Figure 4. Note that in Figure 4, the ML estimator achieves the CRB, and the standard deviation on localization accuracy is less than 3 m for sensor locations within 300 m of the y -axis.

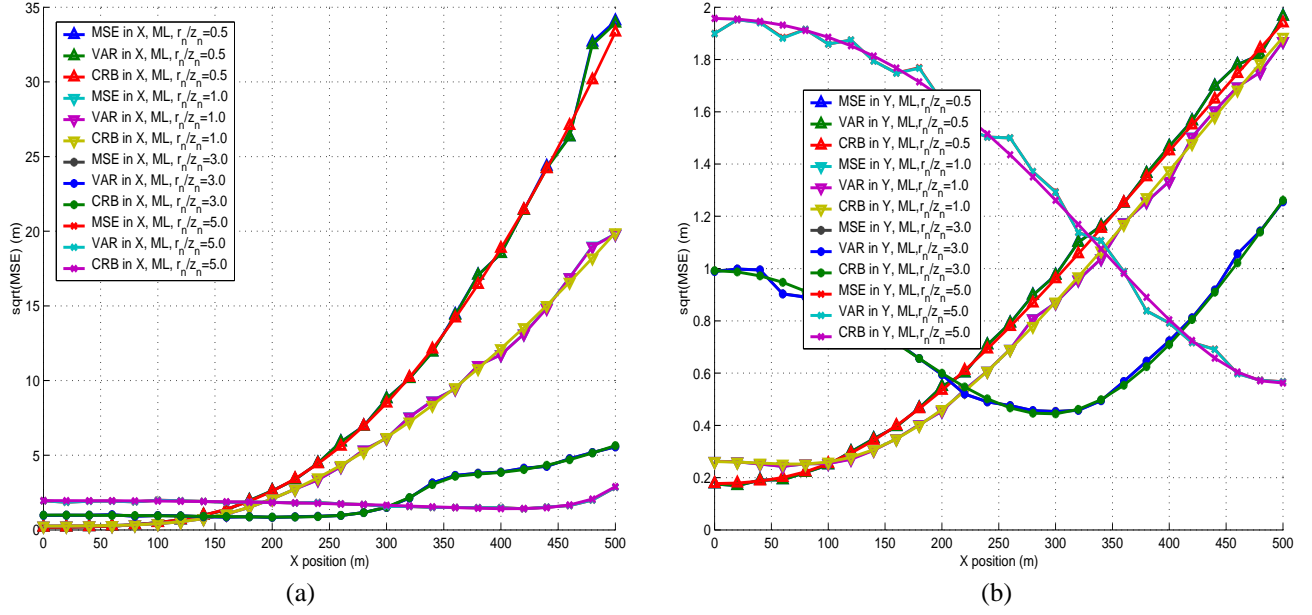


Fig. 3. Sensor location accuracy for AP circular path at elevation $z_n = 100$ m and various radii, with 40 beaconing locations.

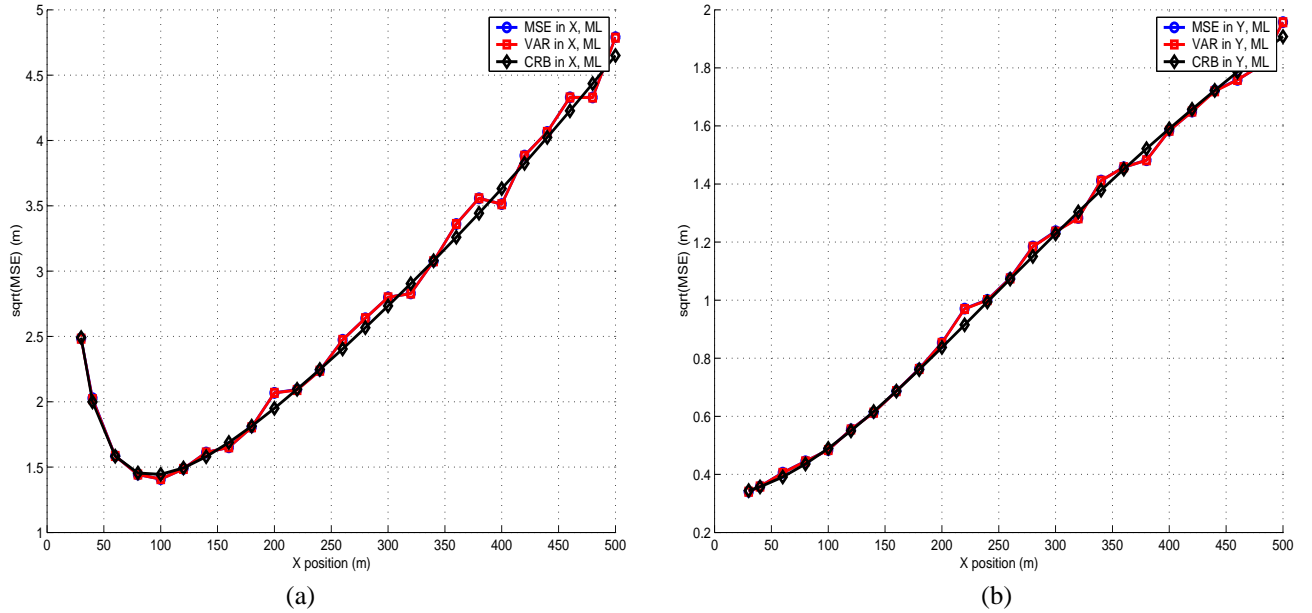


Fig. 4. Sensor location accuracy for AP straight-line path at elevation $z_n = 100$ m and 1,000 m end-to-end distance along y -axis, with 40 beaconing locations.

5. REFERENCES

- [1] R.L. Moses, D. Krishnamurthy, R. Patterson, "A self-localization method for wireless sensor networks," *Eurasip J. Appl. Sig. Proc.*, vol. 4, pp. 348–358, 2003.
- [2] N. Patwari, J.N. Ash, S. Kyperountas, A.O. Hero III, R.L. Moses and N.S. Correal, "Locating the Nodes," *IEEE Signal Processing Magazine*, vol. 22, no. 4, pp. 54–69, July 2005.
- [3] T. R. Damarla, V. Mirelli, "Sensor localization using helicopter acoustic and GPS data," *Proc. of SPIE*, vol. 5417, pp. 336–340, April 2004.
- [4] R. J. Kozick, B. M. Sadler, "Performance of Doppler estimation for acoustic sources with atmospheric scattering," *Proc. IEEE ICASSP'04*, pp. 381–384, May 2004.
- [5] R.J. Kozick and B.M. Sadler, "Sensor localization using acoustic Doppler shift with a mobile access point," *Proc. 2005 IEEE Workshop on Stat. Sig. Proc. (SSP '05)*, Bordeaux, France, July 17–20, 2005.
- [6] M. Karan, R.C. Williamson, and B.D.O. Anderson, "Performance of the maximum likelihood constant frequency estimator for frequency tracking," *IEEE Trans. on Signal Processing*, Vol. 42, No. 10, pp. 2749–2757, Oct. 1994.
- [7] P. M. Djuric and S. M. Kay, "Parameter Estimation of Chirp Signals," *IEEE Trans. on Acoust., Speech, and Signal Processing*, vol. 38, no. 12, pp. 2118–2126, Dec. 1990.
- [8] R.L. Streit and R.F. Barrett, "Frequency line tracking using hidden Markov models," *IEEE Trans. on Acoust., Speech, and Signal Processing*, vol. 38, iss. 4, pp. 586–598, Apr. 1990.
- [9] O. Cramer, "The variation of the specific heat ratio and the speed of sound in air with temperature, pressure, humidity, and CO₂ concentration," *J. Acoustic Soc. of Amer.*, vol. 93, no. 5, pp. 2510–2516, May 1993.
- [10] S.M. Kay, *Fundamentals of Statistical Signal Processing: Estimation Theory*, Prentice-Hall, 1993.
- [11] P. Stoica and T.L. Marzetta, "Parameter estimation problems with singular information matrices," *IEEE Trans. on Signal Processing*, Vol. 49, No. 1, pp. 87–90, Jan. 2001.

Sensor Localization Using Radio & Acoustic Transmissions from a Mobile Access Point

Richard J. Kozick
Bucknell University

Chin-Chen Lee
Cornell University

Brian M. Sadler
Army Research Lab

Lang Tong
Cornell University

Sensor Localization: Overview

- Many applications require known location & orientation of nodes (e.g., source tracking)
- Sensor node deployments:
 - Hand placement, with GPS (or, GPS at nodes)
 - Random placement, air drop, etc.
 - Nodes may be mobile
- Approaches to sensor node localization:
 - Beacons within the network [Moses *et al.*, 2002-2005]
 - Tracking the angle of a moving source
 - ♦ Noncooperative source [Cevher and McClellan, 2001]
 - ♦ Experiments w/ cooperative source [Damarla and Mirelli, 2003-2004]
 - ♦ Cooperative source [Cevher and McClellan, 2006]
 - *Cooperative* mobile access point (AP) w/ *multimodal* transmission

Outline

- Multimodal sensor localization w/ mobile AP
 - Signal proc. options at nodes: Doppler, TOA, AOA
 - Multimodal: radio and acoustics
 - AP broadcasts, so no comms. network required
 - Saves node energy by exploiting external assets
- Focus on narrowband Doppler (acoustic)
 - Measurement model, incl. turbulent scattering
 - Monte-Carlo simulation examples
 - ◆ RMSE localization accuracy & Cramer-Rao bound (CRB)
 - Results: Localization accuracy < 1 m
(in “sweet spot” of AP path)

Sensor Localization: Some Approaches

- Beacons within the network [Moses et. al.]
 - No external assets required
 - Need at least 2 beacons (unknown locations, times)
 - Nodes measure TOA / AOA
 - Network clock sync req'd
 - Network comms req'd
 - ➔ Central Info. Processor
 - TOA / AOA are acoustic
 - Radio for comms.
- Tracking AOAs of a moving source [Cevher and McClellan]
 - Exploits external source w/ motion along straight line
 - Source trajectory is unknown [2001] and known [2006]
 - Nodes (array) track AOAs
 - ➔ Find location & orientation
 - Network clock sync. & comms. are req'd [2001]; not for [2006]
- Experiments with a cooperative helicopter [Damarla & Mirelli, 2003; Cevher & McClellan, 2006]

Sensor Localization:

Multimodal w/ Mobile Access Point

- Exploit external, mobile AP (during deployment, or after)
 - AP knows its position & velocity (e.g., helicopter w/ GPS)
 - AP broadcasts to sensors in two modes
 - ♦ Radio: Timing, AP location & motion, acoustic signal parameters
 - ♦ Acoustic: Inherent platform noise, or synthetic (tone, PN)
- Network clock sync. & comms. are *not* req'd (each node self-localizes, based on the broadcast)
- Signal proc. at nodes: Doppler (NB & WB), TOA, AOA
- AP can provide many beaconing positions (as opposed to fixed beacon locations within the network)
- Accommodates new network nodes & node motion
- Saves node energy (due to mobile AP)

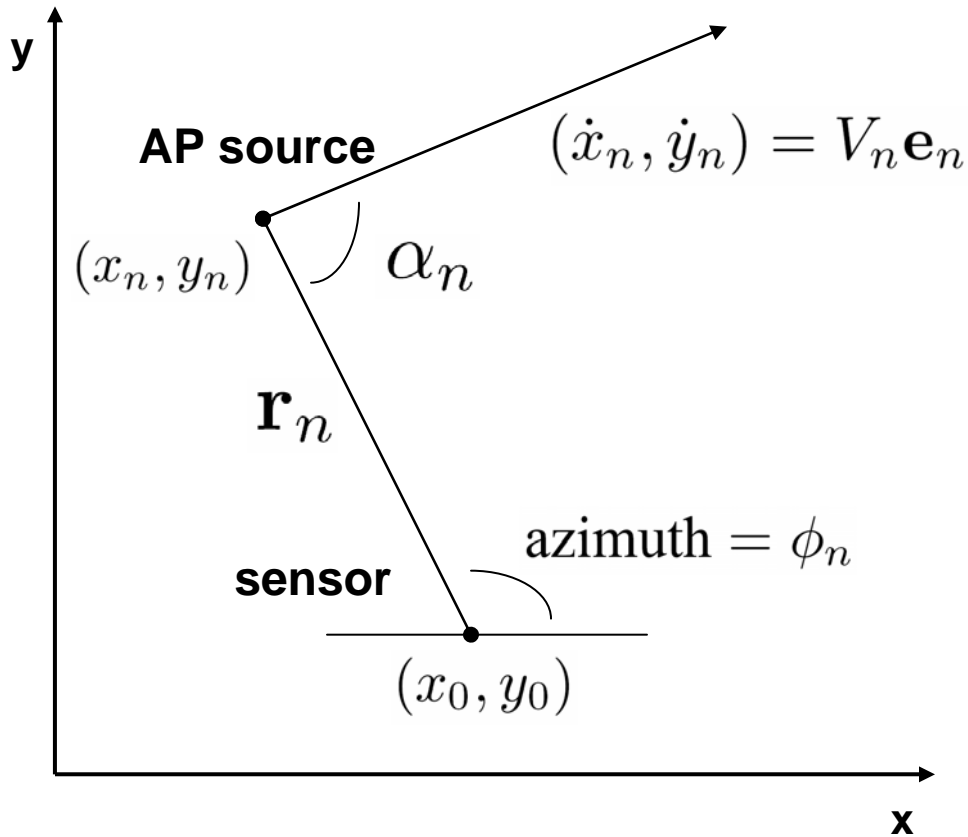
Why Multimodal?

- If use radio alone for Doppler, TOA, AOA
 - Doppler shifts are small at RF for slow platforms
 - TDE requires more sophisticated radio ($> BW$)
 - AOA requires antenna array
 - ➔ Not compatible with low-power, simple radio
- If use acoustics alone for Doppler, TOA, AOA
 - Nodes must communicate to establish network timing (or perform TDOA)
- Combining radio and acoustics
 - Reduces communication ➔ saves energy at nodes
 - Simplifies the signal processing for node localization (known AP location, acoustic Doppler/TOA/AOA)

Acoustic Doppler Shift

- Mobile AP emits acoustic tone
 - Node knows AP location, heading, & tone frequency
 - Simple processing at node (spectral line estimation)
- Can combine Doppler with TOA and/or AOA (not considered here)
- Next:
 - Model for acoustic Doppler shift (incl. atmospheric turbulence effects)
 - Monte-Carlo simulation examples:
 - ◆ Sensor localization accuracy, RMSE and CRBs
 - ◆ Various AP paths

Geometry for Doppler Model



Doppler relations

$$\begin{aligned}
 f_n &= f_s \left(1 + \frac{V_n \cos \alpha_n}{c} \right) \\
 &= f_s + \left(\frac{f_s}{c} \right) \frac{(x_o - x_n) \dot{x}_n + (y_o - y_n) \dot{y}_n}{\left[(x_o - x_n)^2 + (y_o - y_n)^2 \right]^{1/2}} \\
 &= f_s + \left(\frac{f_s}{c} \right) g(\mathbf{x}_o; \mathbf{x}_n, \dot{\mathbf{x}}_n).
 \end{aligned}$$

AP transmits location, velocity vector, and f_s

Sensor Localization from Doppler

- With N Doppler shift measurements (different AP locations)

$$\Delta f_n = \left(\frac{f_s}{c} \right) g(\mathbf{x}_o; \mathbf{x}_n, \dot{\mathbf{x}}_n) + \epsilon_n, \quad n = 1, \dots, N.$$

- Each node solves for its own location (nonlinear LS)

$$\hat{\mathbf{x}}_o = \arg \min_{\mathbf{x}_o} \sum_{n=1}^N \frac{1}{\sigma_n^2} \left[\Delta f_n - \frac{f_s}{c} g(\mathbf{x}_o; \mathbf{x}_n, \dot{\mathbf{x}}_n) \right]^2$$

- Study localization accuracy with respect to
Path of AP
Doppler measurement accuracy, which depends on
Range, frequency, weather (turbulence, Ω), SNR
→ ϵ_n Gaussian, physics-based model for σ_n^2

Cramer-Rao Bound (CRB) and AP Path Analysis

Fisher Information Matrix (FIM):

$$\mathbf{J}(\mathbf{x}_0|\mathcal{P}) = \sum_{n=1}^N \frac{1}{\sigma_n^2} \left(\frac{\partial \Delta f_n}{\partial \mathbf{x}_0} \right) \left(\frac{\partial \Delta f_n}{\partial \mathbf{x}_0} \right)^T \quad \frac{\partial \Delta f_n}{\partial \mathbf{x}_0} = \frac{f_s}{c} \frac{1}{r_n} \left(\dot{\mathbf{x}}_n - \frac{(\dot{\mathbf{x}}_n^T \tilde{\mathbf{r}}_n)}{r_n^2} (\mathbf{x}_0 - \mathbf{x}_n) \right)$$

Set of unlocalizable

sensor positions: $\mathcal{X}(\mathcal{P}) = \{\mathbf{x} \mid \det(\mathbf{J}(\mathbf{x}|\mathcal{P})) = 0\}$

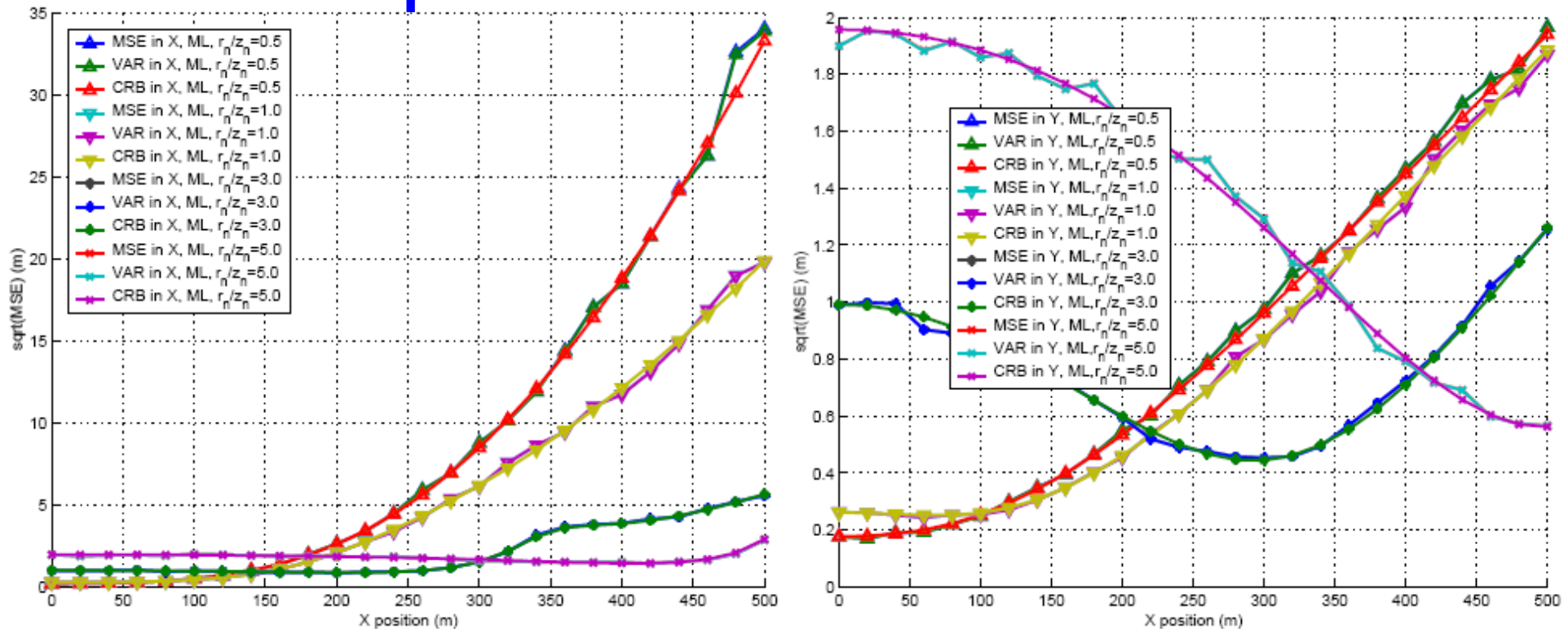
Straight-line, constant velocity AP path:

→ χ = line directly under AP path

Example 1: Circular AP Path

- AP travels in circular path around origin:
 - Elevation 100 m
 - Speed = 33.5 m/s = $c/10$
 - Various radii
 - $N = 40$ beaconing positions (equally spaced)
 - Acoustic tone frequency $f_s = 100$ Hz
- Sensor location: $\mathbf{x}_o = (x, 0)$, vary x

Example 1: Circular AP Path



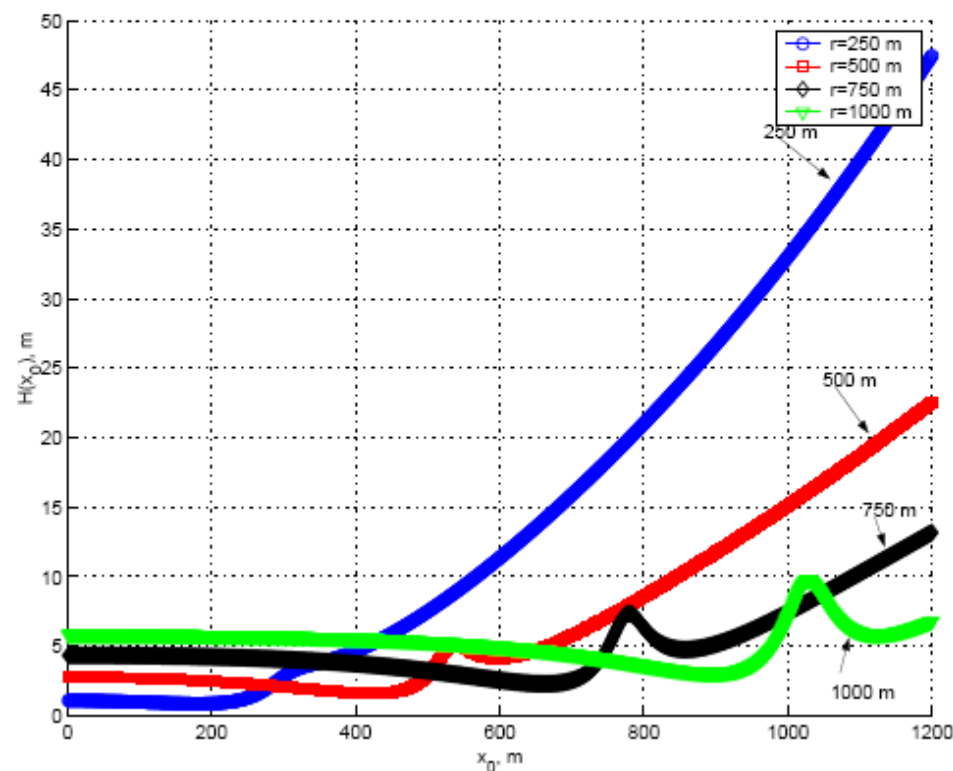
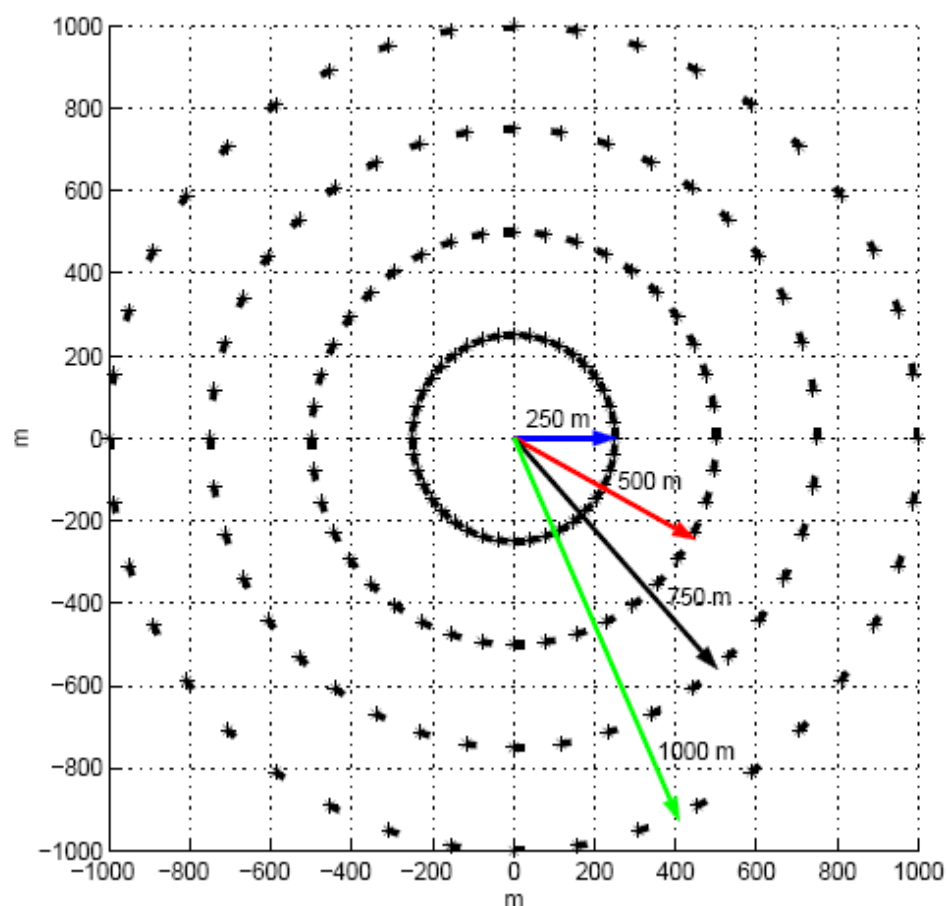
Localization accuracy ~ 1 m (and less) when sensor is inside circle

Tradeoff in AP path radius and sensor localization accuracy

RMSE = CRB for all sensor locations \rightarrow Justifies study of CRB

CRBs for Circular AP Paths

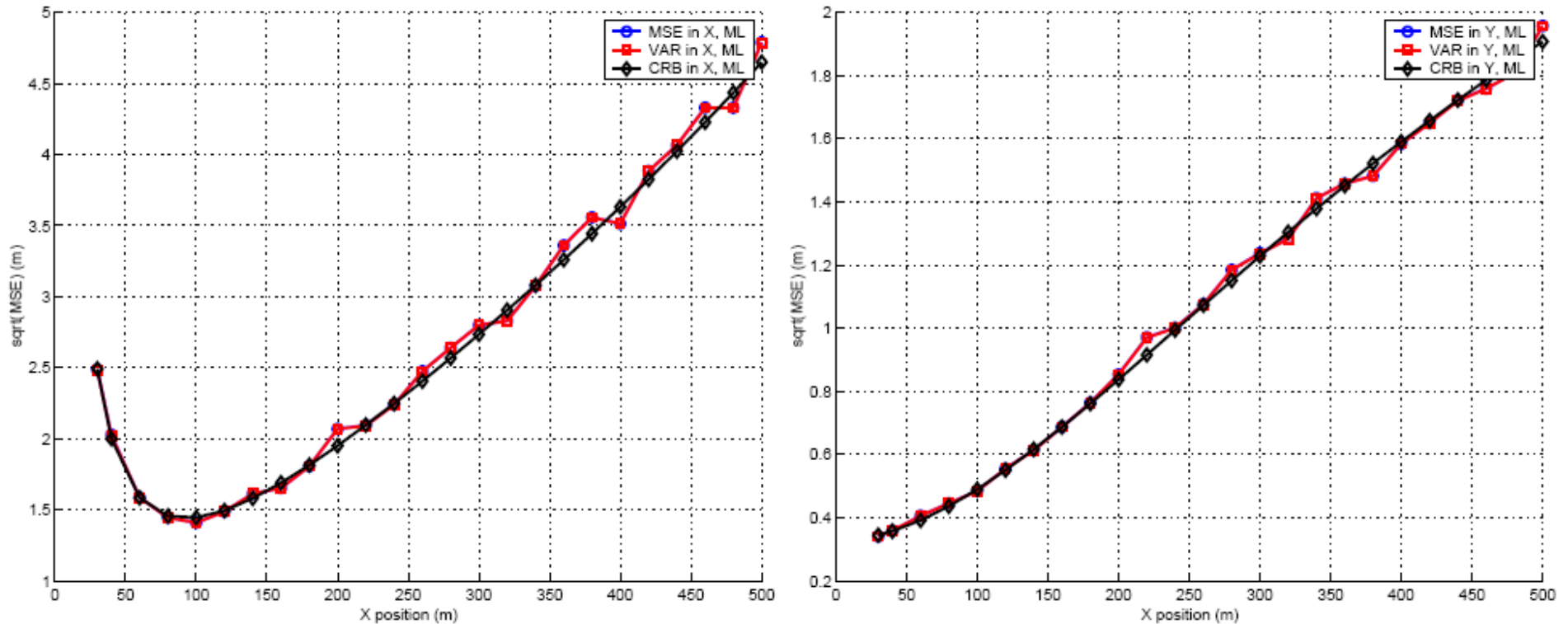
$$\mathcal{H}(\mathbf{x}_0) \triangleq [\text{trace}(\mathbf{I}^{-1}(\mathbf{x}_0))]^{1/2}$$



Example 2: Straight-Line AP Path

- AP travels in straight-line path over y-axis:
 - Elevation 100 m
 - Speed = 33.5 m/s = $c/10$
 - End-to-end distance 1,000 m ($y=-500$ to $+500$)
 - $N = 40$ beaconing positions (equally spaced)
 - Acoustic tone frequency $f_s = 100$ Hz
- Sensor location: $\mathbf{x}_o = (x, 0)$, vary x

Example 2: Straight-Line AP Path



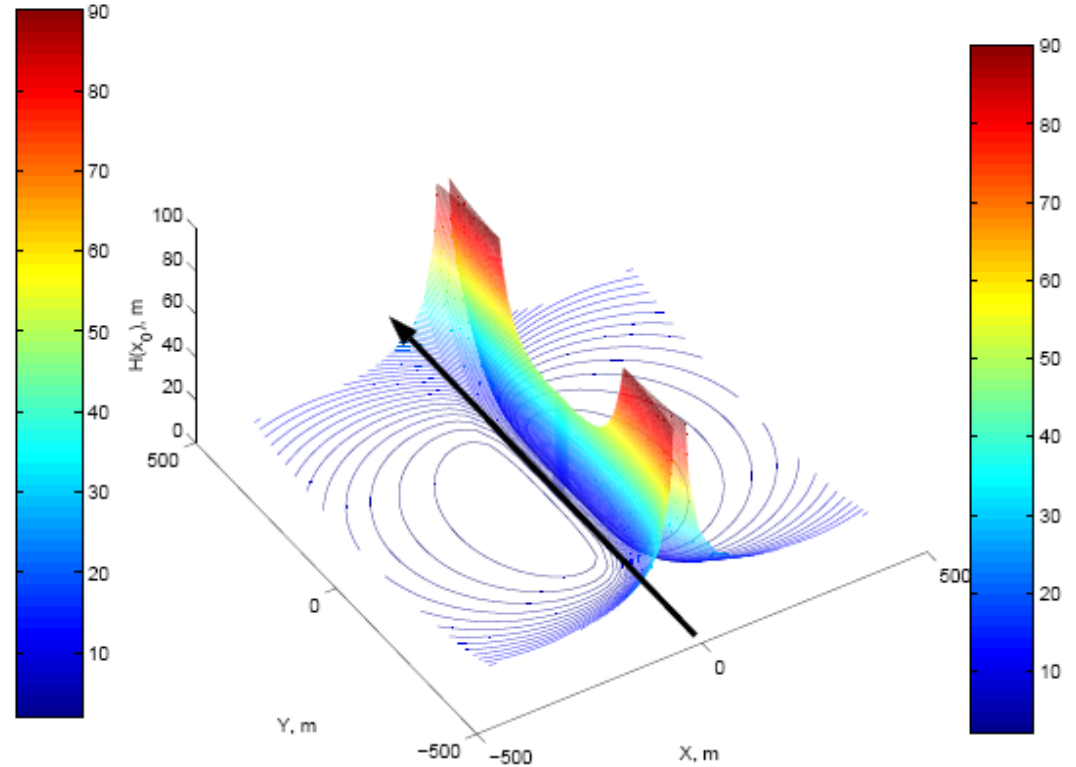
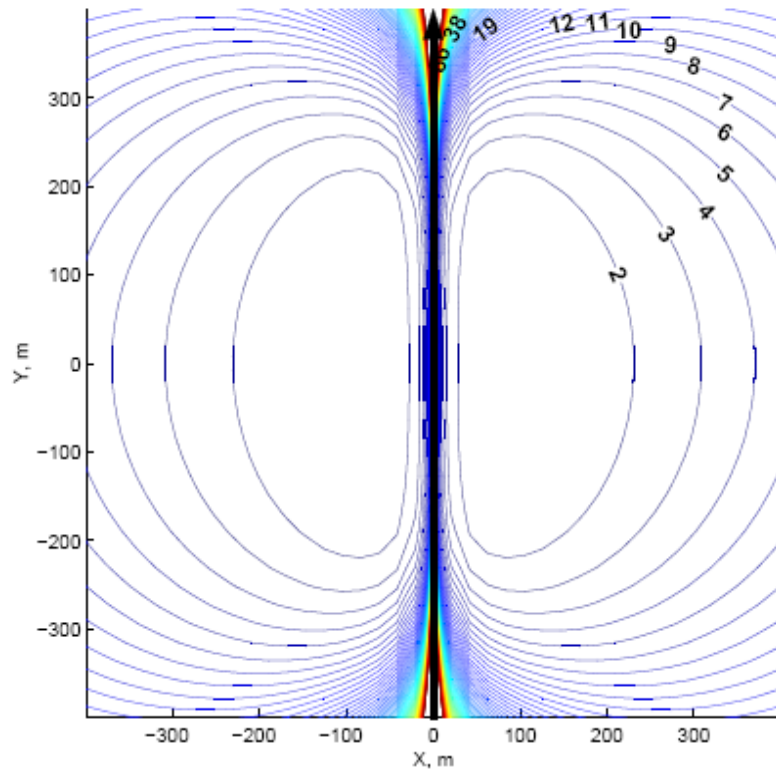
Localization accuracy ~ 1 m (and less) when sensor is inside circle

Unlocalizable for $x=0$, “best” location is $x=100$ m

RMSE = CRB for all sensor locations

CRBs for Straight-Line AP Paths

$$\mathcal{H}(\mathbf{x}_0) \triangleq [\text{trace}(\mathbf{I}^{-1}(\mathbf{x}_0))]^{1/2}$$



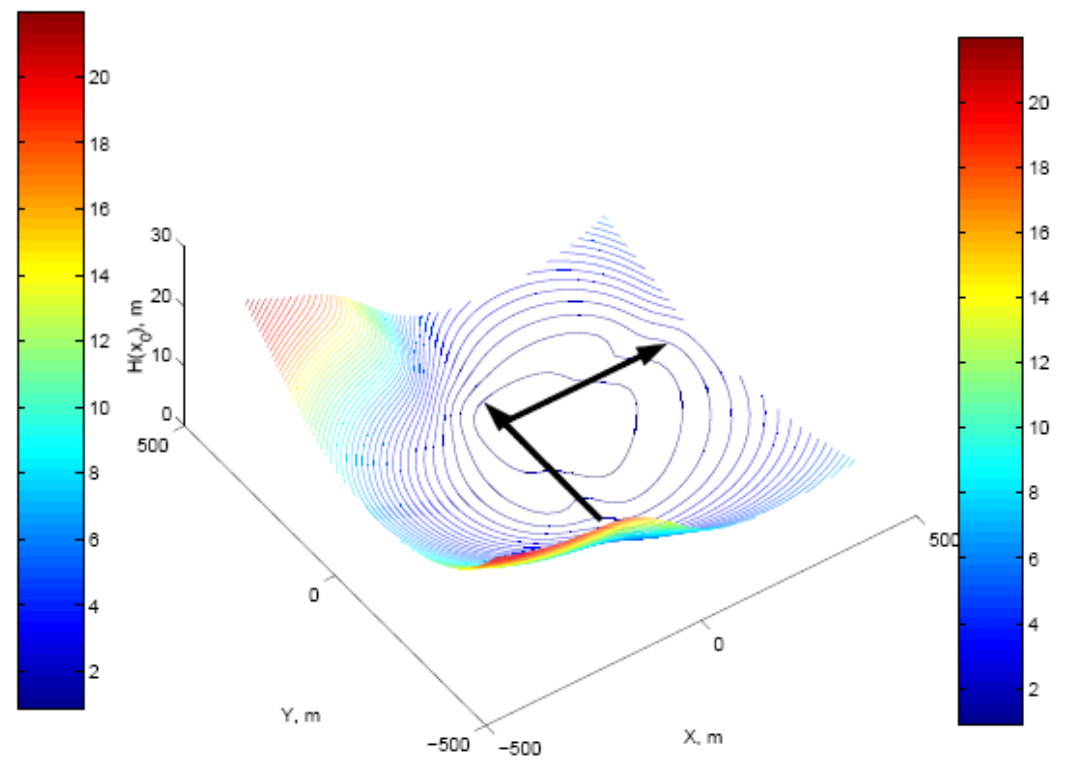
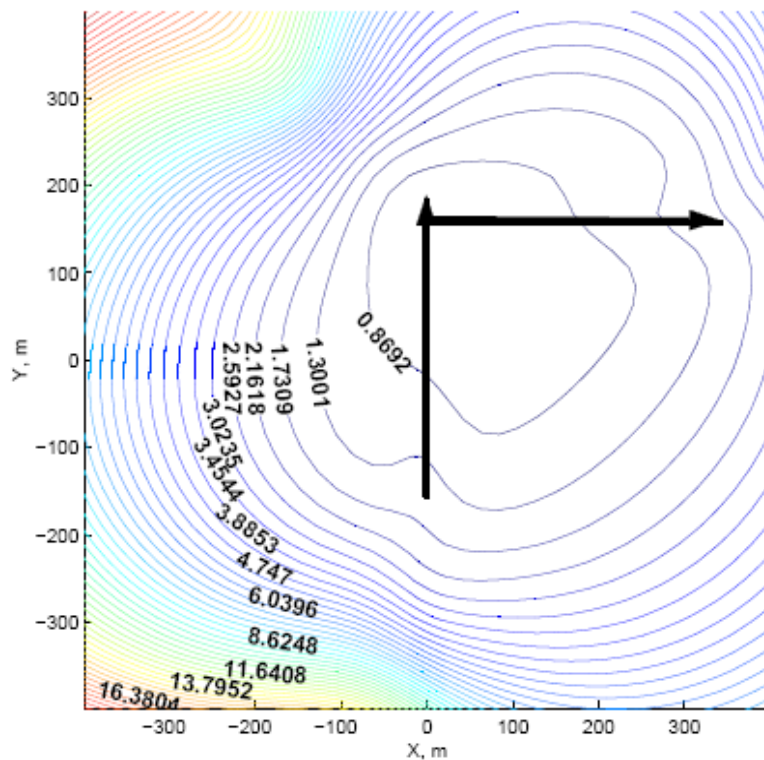
End-to-end distance = 447 m

CRBs for Other AP Paths

- Turn after straight-line path (right angle)
→ No points of unlocalizability
- Semi-circular path
- Circular path
- All enable similar localization accuracy

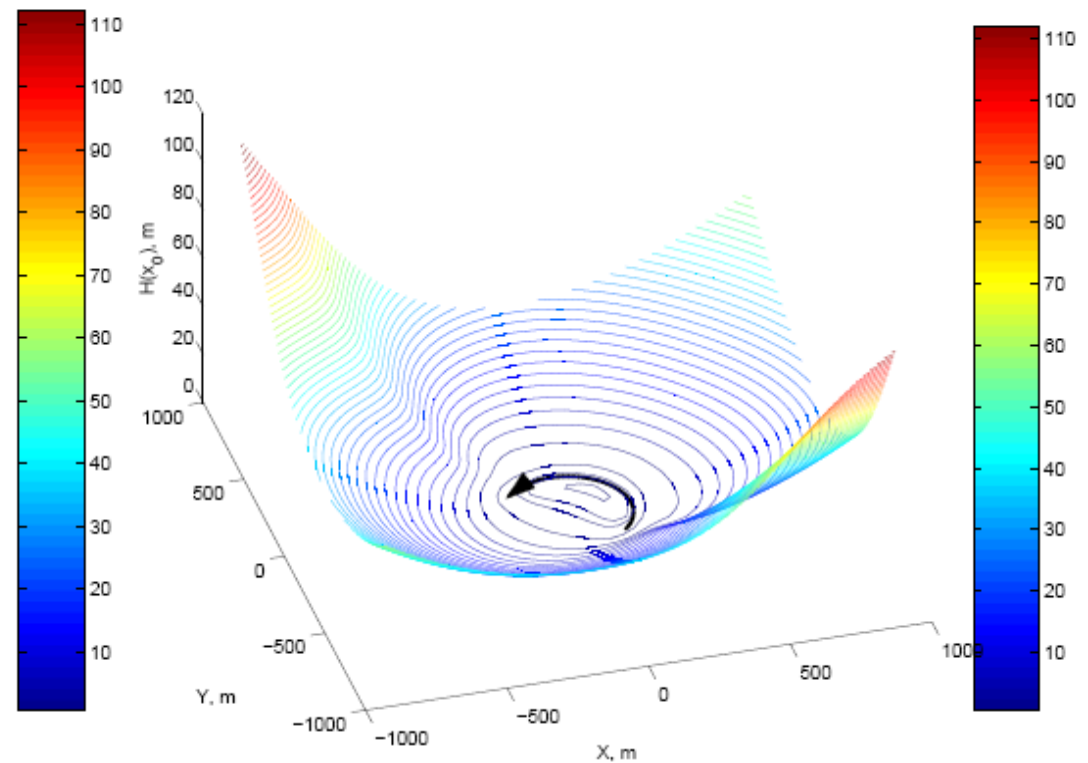
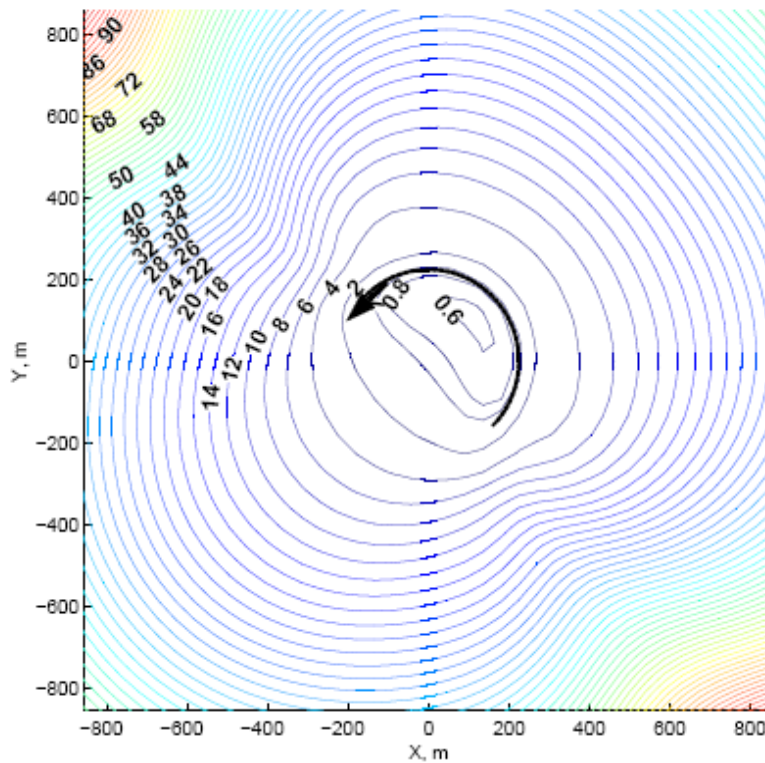
Two Straight-Line Paths

$$\mathcal{H}(\mathbf{x}_0) \triangleq [\text{trace}(\mathbf{I}^{-1}(\mathbf{x}_0))]^{1/2}$$



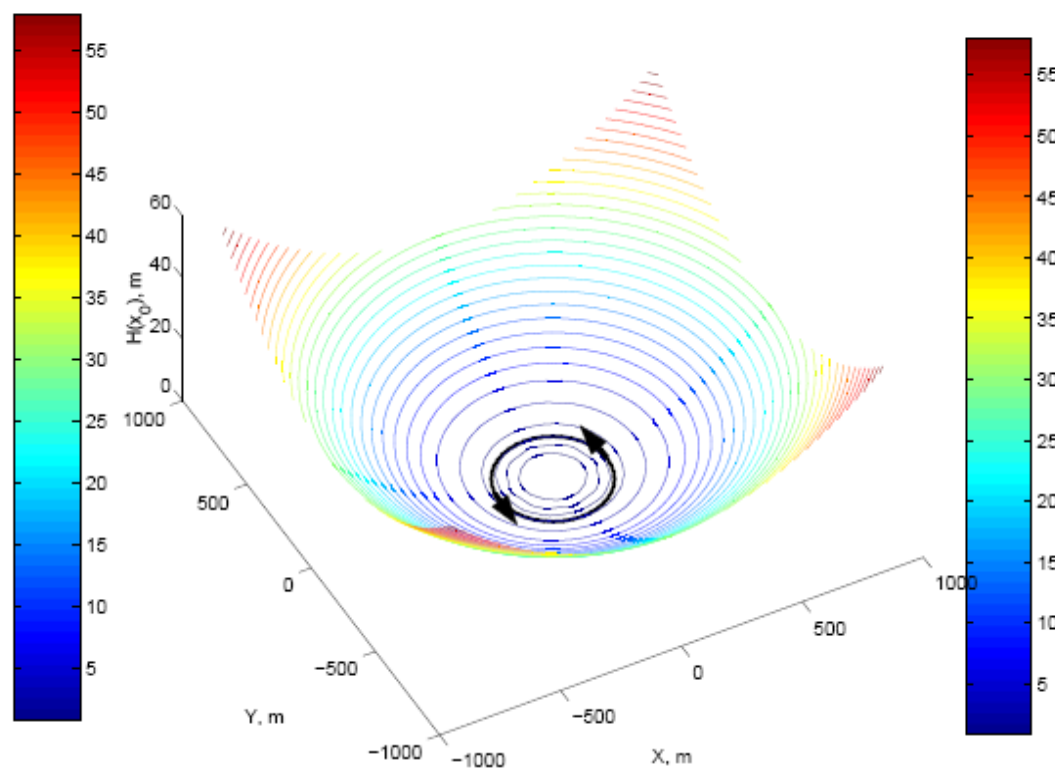
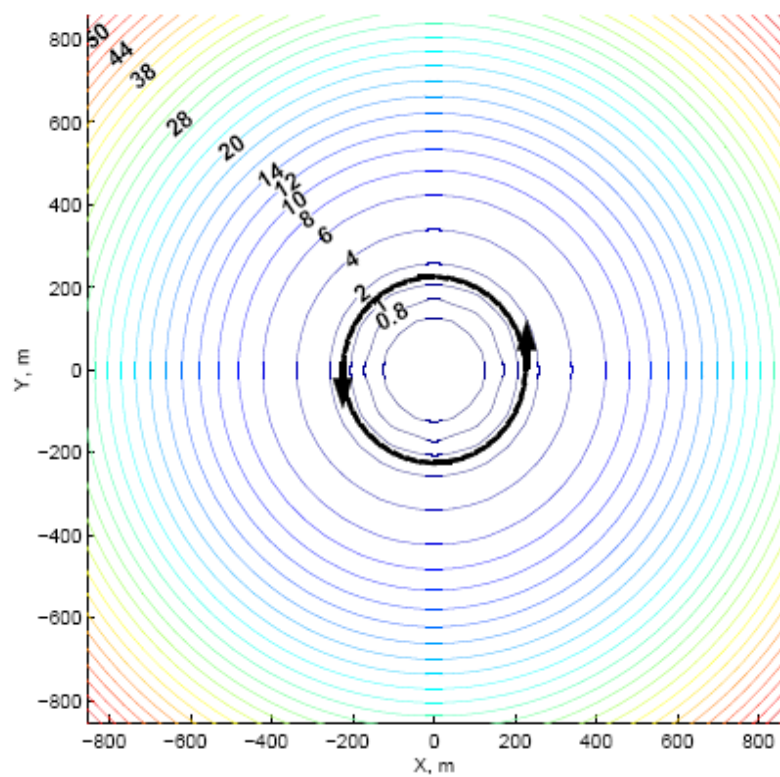
Semi-Circular Path

$$\mathcal{H}(\mathbf{x}_0) \triangleq [\text{trace}(\mathbf{I}^{-1}(\mathbf{x}_0))]^{1/2}$$



Circular Path

$$\mathcal{H}(\mathbf{x}_0) \triangleq [\text{trace}(\mathbf{I}^{-1}(\mathbf{x}_0))]^{1/2}$$



Concluding Remarks

- Features of sensor localization with mobile AP:
 - Signal processing options (Doppler, TOA, AOA)
 - AP can beacon from many positions
 - Multimodal AP broadcasts, so
 - ♦ Localize many sensors simultaneously
 - ♦ Network comms. *not* req'd → saves node energy
 - ♦ Simpler processing at node
 - Accommodate new nodes and node motion
- Simulations → Accuracy < 1 m (“best” locations)
- Results excluded here:
 - Ignoring turbulence is optimistic by orders of mag.
 - Analyzed source motion effects (varying Doppler shift)
- Study TOA, AOA, and combinations with Doppler